Available online at www.sciencedirect.com
SCIENCE DIRECT
Tectonophysics 416 (2006) 33–52
TECTONOPHYSICS
www.elsevier.com/locate/tecto

Upper mantle structure of the Northern Eurasia from peaceful nuclear explosion data

G.A. Pavlenkova, N.I. Pavlenkova *

Institute of Physics of the Eart, Moscow, Russia

Received 24 February 2005; accepted 28 November 2005
Available online 7 February 2006

Abstract

Several long-range seismic profiles were carried out in Russia with Peaceful Nuclear Explosions (PNE). The data from 25 PNEs recorded along these profiles were used to compile a 3-D upper mantle velocity model for the central part of the Northern Eurasia. 2-D crust and upper mantle models were also constructed for all profiles using a common methodology for wavefield interpretation. Five basic boundaries were traced over the study area: N1 boundary (velocity level, $V=8.35$ km/s; depth interval, $D=60$–130 km), N2 ($V=8.4$ km/s; $D=100$–140 km), L ($V=8.5$ km/s; $D=180$–240 km) and H ($V=8.6$ km/s; $D=300$–330 km) and structural maps were compiled for each boundary. Together these boundaries describe a 3-D upper mantle model for northern Eurasia. A map characterised the velocity distribution in the uppermost mantle down to a depth of 60 km is also presented. Mostly horizontal inhomogeneity is observed in the uppermost mantle, and the velocities range from the average 8.0–8.1 km/s to 8.3–8.4 km/s in some blocks of the Siberian Craton. At a depth of 100–200 km, the local high velocity blocks disappear and only three large anomalies are observed: lower velocities in West Siberia and higher velocities in the East-European platform and in the central part of the Siberian Craton. In contrast, the depths to the H boundary are greater beneath the craton and lower beneath in the West Siberian Platform. A correlation between tectonics, geophysical fields and crustal structure is observed. In general, the old and cold cratons have higher velocities in the mantle than the young platforms with higher heat flows.

Structural peculiarities of the upper mantle are difficult to describe in form of classical lithosphere–asthenosphere system. The asthenosphere cannot be traced from the seismic data; in contrary the lithosphere is suggested to be rheologically stratified. All the lithospheric boundaries are not simple discontinuities, they are heterogeneous (thin layering) zones which generate multiphase reflections. Many of them may be a result of fluids concentrated at some critical P–T conditions which produce rheologically weak zones. The most visible rheological variations are observed at depths of around 100 and 250 km.

Keywords: Upper mantle; Seismic studies; Nuclear explosions; Siberia

1. Introduction

The paper includes collection of results and systematic analysis of voluminous materials produced during the last 25–30 years when the seismic investigations with large chemical explosions and Peaceful Nuclear Explosions (PNE) were conducted in Russia. Several super long-range profiles were carried out with PNEs specially designed for this research (Fig. 1). They were parts of a regular network of the Deep Seismic Sounding (DSS) coverage of the USSR territory, and were acquired by GEON Centre of the Ministry

* Corresponding author. Tel.: +7 95 254 23 27; fax: +7 95 255 60 40.
E-mail address: ninapav@ifz.ru (N.I. Pavlenkova).

0040-1951/$ - see front matter © 2006 Elsevier B.V. All rights reserved.
doi:10.1016/j.tecto.2005.11.010

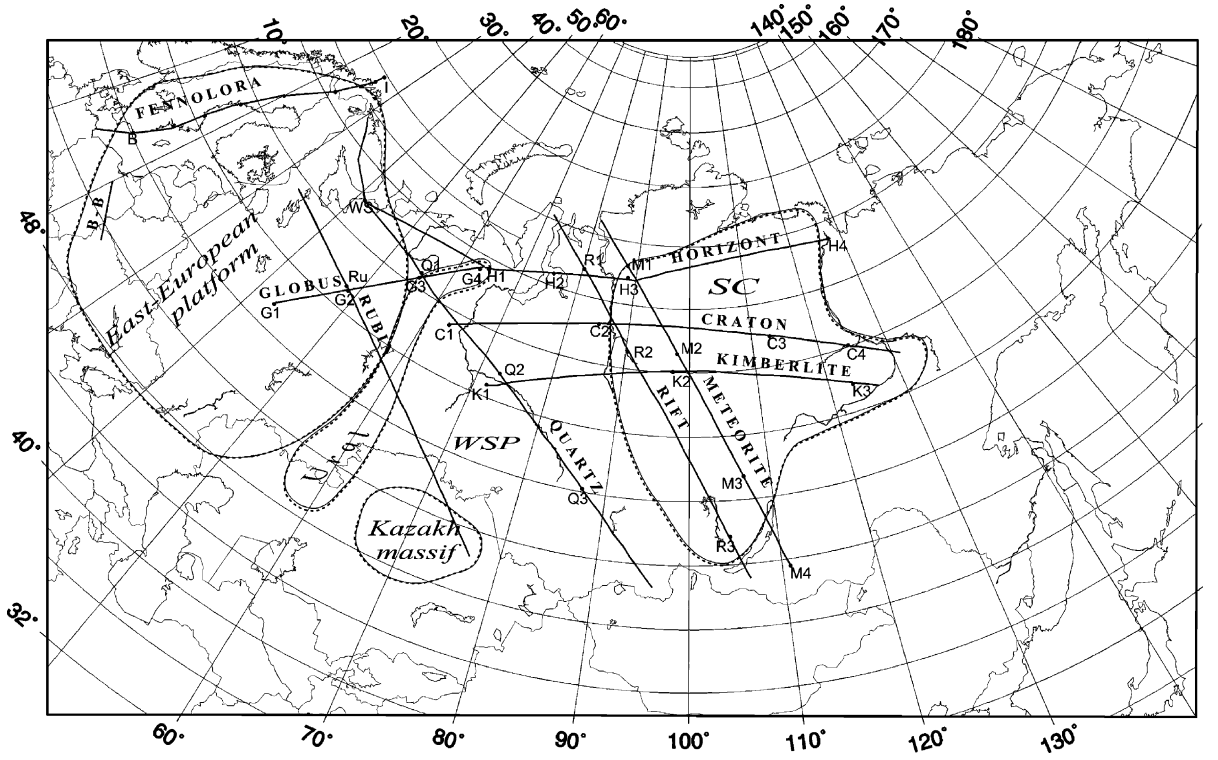

Fig. 1. Map showing the location of the long-range seismic profiles in the Northern Eurasia. Shadow zones show the East-European Platform and the Siberian Craton (SC). WSP—West-Siberian Platform, T-P—Timan-Pechora Plate. Letters indicate location of the shots used in the interpretation, Peace Nuclear Explosion (PNE): Q1, Q2, Q3 and WS along the profile Quartz, G1, G2, G3 and G4—along the profile Globus; H1, H2, H3 and H4—along the profile Horizont; C1, C2, C3 and C4—along the profile Craton; K1, K2 and K3 along the profile Kimberlite; R1, R2 and R3 along the profile Rift; M1, M2, M3 and M4 along the profile Meteorite; Ru along the profile Rubin; large chemical explosions B and I along the profiles Fennolora and B-B.

of Natural Resources of Russia in the 1960–1980s (Benz et al., 1992; Egorkin, 1999; Fuchs, 1997).

All the profiles were coupled with seismic research, which included 3-component analogue recordings of chemical and PNE shots at a large number of stations positioned on profiles with a 10-km station spacing. The length of the profiles varies from 1500 to 3000 km, shot points (SP) intervals between the chemical explosions are of 100–150 km. The number of PNEs varies from one on the Rubin (SP Ru in Fig. 1) to four on the Craton (SPs C1–C4) and Globus (SRs G1–G4) profiles. The large chemical explosions provided recordings up to 300–600 km offsets, the PNE—up to 3200 km offsets. Both types of the explosions provided high quality only P-wave phases.

The first interpretation of the data was made by GEON Centre and crustal models were constructed from the chemical explosion records for all profiles. The PNE data was processed in GEON mainly during the last decade. However, only part of the results was published (Egorkin and Chernyshov, 1983; Egorkin et al., 1987; Egorkin, 1997, 1999). Some PNE data were also interpreted at the Institute of Physics of the Earth (Pavlenkova, 1996a; Pavlenkova et al., 1996).

During the last years, some PNE data have become available to international groups. The Quartz, Rift and Craton profiles were discussed in many publications: Quartz (Mechie et al., 1993; Riberg et al., 1996; Morozov et al., 1999), Rift (Cipar et al., 1993; Priestly et al., 1994; Pavlenkova et al., 2002), Craton (Egorkin, 1997; Nielsen et al., 1999). Some profiles Globus, Rubin, Horizont, White Sea-Vorkuta are not interpreted yet or not published. General analyses of the data and their comparison with the other long-range seismic profiles were made in Pavlenkova (1996a), Fuchs (1997) and Egorkin (1999). In this paper, we present results of the systematic analysis of all PNE records and interpretation of the unpublished data and reinterpretation of all other data, including the Fennolora profile (Guggisberg and Berthelsen, 1987; Abramovitz et al., 2002), in the form of 2-D and 3-D velocity models of the upper mantle.

The reinterpretation was necessary because the velocity models of the various authors differ, and it is

difficult to understand if the differences are a result of non-uniqueness of the seismic data interpretation or a result of the different methodology used. Some previous models were based only on a part of the data available. For example, the chemical explosions were not used for the uppermost mantle modelling and only small part of the secondary arrivals was included in the interpretation. As a result, some authors show many boundaries and many inversion zones (Egorkin and Chernyshov, 1983; Egorkin et al., 1987; Morozov et al., 1999), and other authors present very simple models (Nielsen et al., 1999). Besides the models are presented in different forms and it is difficult to use them for compilation of 3-D velocity models.

We have reinterpreted all the data using the same methodology for the wave field analysis and 2-D velocity modelling. All models are presented in a common form. They characterise only the upper mantle structure. Regarding the mantle transition zone, there is not enough data to compile a 3-D velocity model. The transition zone boundaries are traced in the narrow central portion of the Siberian Craton and, only along the Craton profile they are determined from the reversed shots (Egorkin, 1997).

The goal of this study is to use the wave analysis and the 2-D and 3-D velocity models to identify the principal regularities in upper mantle velocity structure and to correlate with geological features or geophysical fields of the region. It is interesting also to answer questions such as: Are there regional seismic boundaries in the upper mantle? How does the lithosphere–asthenosphere system look like beneath the platforms? What is the nature of the velocity inhomogeneity and seismic boundaries? What are the differences in the mantle structure between the tectonic units.

The long-range profiles cross several large tectonic futures in the Northern Eurasia: the East European Platform, the Siberian Craton, the Urals, the West Siberian Platform and Timan-Pechora Plate (Fig. 1). The observed wave fields depend on the tectonic features that differ in ages, in geological history, in crustal structure and geophysical fields (Bulina, 1976, Belousov et al., 1991; Pollack et al., 1993).

The East European Platform age is Archean-Proterozoic. Two major tectonic domains are distinguished in the northern part of the platform: the Baltic Shield and the Russian Plate. Crustal thickness changes from 40 to 50 km and average velocity in the consolidated crust is around 6.5 km/s. The platform has a distinctly differentiated and mosaic magnetic field. The heat flow varies only slightly, the average being 40–50 mW/m^2.

The Siberian Craton is of the same Archean-Proterozoic age. Two shields and two large depressions are distinguished in the craton area. The depression in the western part of the craton, the Tunguss Basin, is 8–10 km deep and filled with high-density sediments and with plateau-basalts. In the eastern part of the craton, the 12-km-deep Vilyui Basin is filled with younger sediments. The crustal thickness is of 40–45 km in the Siberian craton, the average velocity is 6.5–6.6 km/s. The magnetic field has sharply differentiated anomalies with different orientations. It is an effect of the plateau-basalts. The heat-flow is much more lower than in the East-European platform: about 30 mW/m^2.

The West-Siberian Platform is of Caledonian and Hercynian ages. It is covered by Mesozoic sediments of 3–15 km of thickness. The crust is slightly thinner than in the old platforms—35–40 km, the average velocities in its consolidated part are 6.5 km/s in the plate area and they increase up to 6.9 km/s beneath deep basins. The magnetic and gravity fields do not differ much from the East-European Platform. The heat flow is more variable and has higher values: 60–65 mW/m^2.

The Timan-Pechora Plate is a small plate between the North Urals and the East European Platform. It is the same age as the West Siberian Plate and it is also covered by thick Mesozoic sediments and has higher heat flow.

The Urals is a Palaeozoic orogen with a specific crustal structure. High density and high velocity material is typical for its upper crust. They may be traced by strong magnetic and gravity anomalies along the whole belt. Clear increasing of the crustal thickness (up to 55 km) is also typical for the Urals (Druzhinin et al., 1981; Carbonel et al., 2000). The heat flow is low, around 30–40 mW/m^2.

2. Observed wave fields and methodology of their analysis and interpretation

To derive 2-D and 3-D velocity models from a large amount of the seismic data, the tomographic method is usually used. Tomography is the fastest method to obtain models but it is not the best one for DSS data interpretation. The method has two significant limitations. It is based mainly on the first arrivals and its basic model is a continuous velocity function without inversions. With DSS, the secondary arrivals are important information on the seismic boundaries (reflectors), which are often the main interest of study. The reflections decrease the non-uniqueness of the velocity model construction and increase the accuracy of depth deter-

mination. The velocity inversions are also important features of the mantle structure, and there is no reason to exclude them from the interpretation.

Our methodology uses all information in the recorded wave fields from both chemical explosions and PNEs to derive consistent solutions in form of 2-D velocity models of the crust and upper mantle along all profiles. The main goals of our interpretation are (1) comparative analysis of all wave fields for determination regular (main) phases, which are possible to pick up in all records, (2) construction of time cross-sections from both first and secondary arrivals in order to determine realistic 2-D starting velocity models, (3) consistent 2-D velocity modelling for all profiles, and (4) compilation of 3-D model in the form of depth maps to seismic boundaries.

The combination of the PNE records together with the chemical ones increases the amount of data on the uppermost mantle structure which is difficult to get from the PNE records alone. Many chemical explosions image the mantle refraction Pn phase up to 500–600 km offsets, and thus, the records may be used for detailed sub-Moho velocity studies. The reflections from the Moho (PmP waves), recorded from the chemical explosions also help to determine the PNE first wave origin at 200–300 km offset, because Pn refractions sometimes have low amplitude and are not visible on the PNE seismograms within the high amplitude reflections from the uppermost mantle boundaries.

The PNE records (Fig. 2) illustrate the complex wave patterns. Strongly different apparent velocities are observed at the longest observation at 2000–2300 km offsets where the velocities of 7.8–8.8 km/s typical for the upper mantle are replaced by the phases with velocities of 10.5–11.5 km/s. These latter waves, well known in seismology, are associated with the mantle transition zone at 400–700 km, so-called 20^0 discontinuity. We have interpreted only the upper mantle waves and waves from the top of the transition zone (P_{410}).

The upper mantle waves also form complex wave fields with many first and secondary phases. Their apparent velocities and amplitudes change with distances and from one profile to another. At far offsets, the first arrivals consist of a combination of secondary phases. Most phases attenuate at some offsets and, as a result, the first arrivals often have stepwise form (RNEs Q2, M4 and R2 in Fig. 2). Such a picture is typical for the reflections or diving waves.

The most important stage of our analysis is the determination of the regular (main) phases which are characterised by high amplitudes and by similar velocities and, which, may be traced in most record-sections. The first arrivals are analysed separately for every shot-point and they are divided into branches with different apparent velocities. Strong changes in amplitudes and, especially, time delays of the first arrivals are marked to trace all visible secondary phases. Main attention is paid to phases that can be correlated for long distances and, can be extended as first arrivals. Those are considered as regular waves and they distinguish the seismic boundaries and constrain the velocities along them. High amplitude secondary arrivals are also identified (Figs. 2 and 3). In the next stage, the wave analysis is continued using the reversed and overlapping records. The travel-times of the waves observed from all shots are compared to find regular features and to determine a general velocity model characteristic for the whole study area.

The records show that observed phases may be approximated by several regular wave groups: Pn, P_{N1}, P_{N2}, P_L and P_H. The Pn waves are recorded in offset interval of 200–1100 km. Their apparent velocities increase slowly from 8.1 to 8.3 km/s. At larger offsets, the P_{N1} and P_{N2} first arrivals have velocities of 8.4–8.5 km/s, recorded within 1100–1600 km offsets. At first, the travel times of these waves were interpreted as a single wave P_N reflected from the N boundary at depth around 100 km. This boundary was identified in many other regions and was considered as a principal boundary in the upper mantle (Pavlenkova, 1996a,b). It corresponds to the 8^0 boundary (Thybo and Perchuc, 1997).

More detailed studies of the PNE wave fields show that the P_N may be divided in two phases: P_{N1} and P_{N2} (Figs. 3 and 4) which correspond to N1 and N2 boundaries. The boundary velocities are close (8.35–8.4 km/s) and their depths differ only in 20–30 km, that is why it was difficult to separate them. A characteristic feature of the P_{N1} is that it is often are recorded after a sharp attenuation (shadow zone) of Pn waves, suggesting the N1 boundary to be the bottom of low velocity layer.

In the 1600–2100 km offset range, the first arrivals have apparent velocities of 8.6–8.7 km/s, the P_L phase. These waves are recorded also as secondary arrivals and they were interpreted as reflections from the L boundary at depths 200–250 km. This boundary is known from seismology as the Lehmann discontinuity. In the offset range of 800–1300 km where P_L waves are observed as secondary arrivals, they display relative high amplitudes (PNE Q2 in Fig. 2). These arrivals often expand the coda of P_{N2} making it difficult to differentiate between them (PNE C2 in Fig. 2).

The P_H waves are recorded mainly as secondary arrivals at the distances of 1700–2200 km (Fig. 3). The first identification of these phases was made by

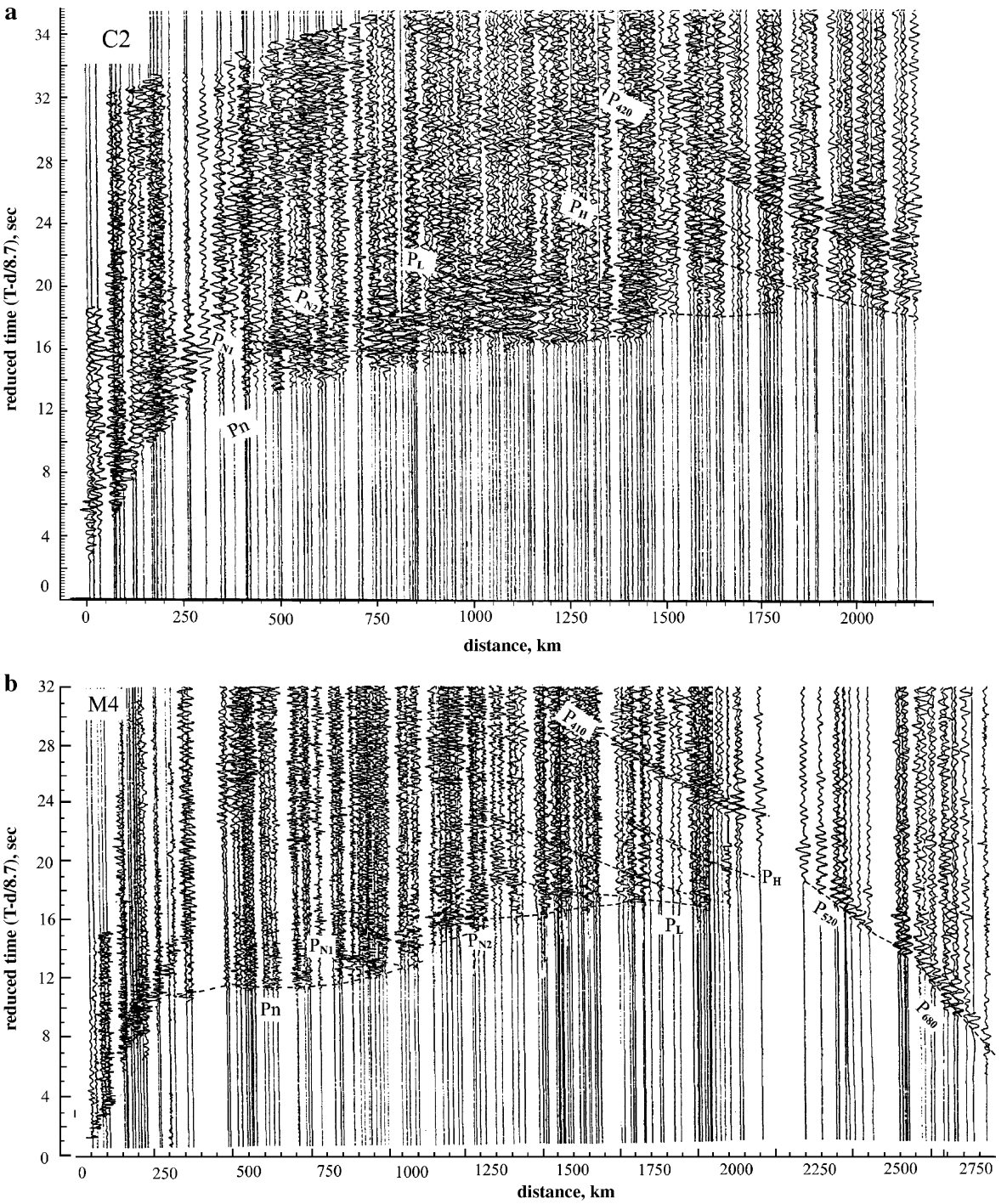

Fig. 2. Record-sections of the upper mantle waves from the PNEs: (a) C2 along Craton profile, (b) M4 along Meteorite profile, (c) Q2 along Quarts profile, and (d) R2 along Rift. In a–d, the reduction velocity is 8.7 km/s. The main mantle waves which were traced in all records: Pn—refraction in the uppermost mantle (apparent velocities Va=8.0–8.5 km/s), P_{N1} (Va=8.2–8.5 km/s), P_{N2} (Va=8.3–8.6 km/s), P_L (Va=8.6–8.8 km/s) and P_H (Va=8.8–9.0 km/s) are reflections and refractions from the corresponding seismic boundaries N1, N2, L and H. In addition, P_{410}, P_{520} and P_{680}-waves from the boundaries of the mantle transition zone at depths 410, 520 and 680 km were observed.

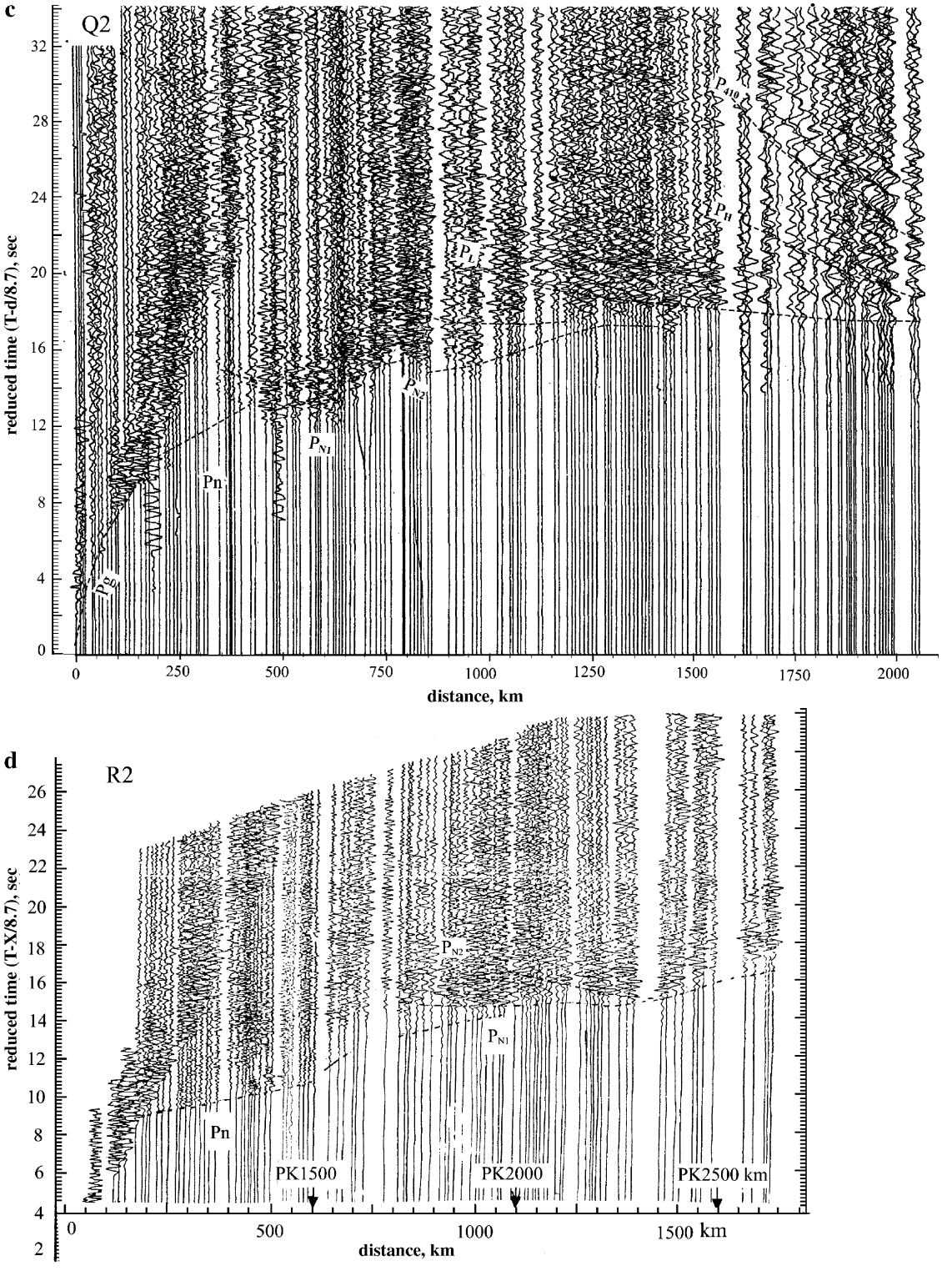

Fig. 2 (*continued*).

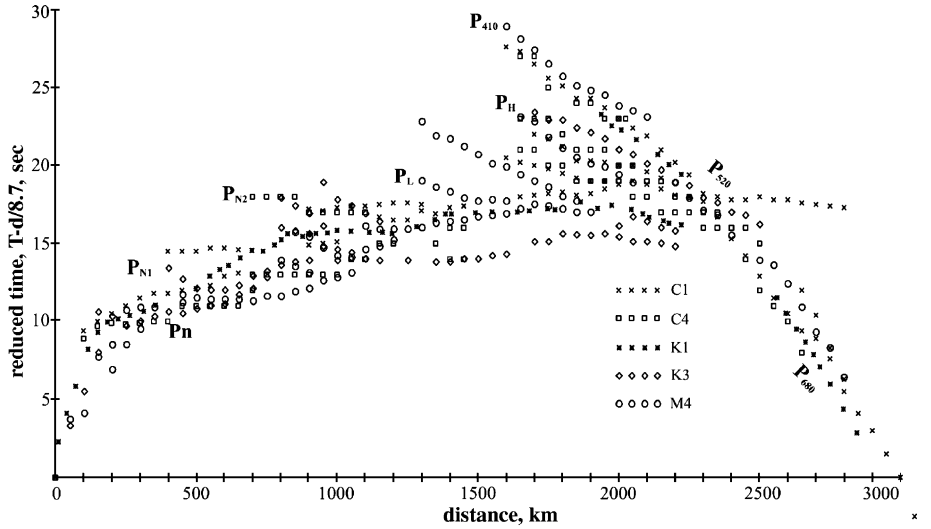

Fig. 3. Travel-times of the main waves recorded from PNEs C1, C4, K1, K3 and M4 (location in Fig. 1). Reduction velocity is 8.7 km/s.

Thybo et al. (1997) where the waves are called P_{350}. Due to the coda length and complex nature of this arrival it is difficult to determine depths of the correspondent reflector, we labelled the wave as P_H. Usually, these waves are weak in most record-sections. However, sometimes, the reflections from the H boundary are so strong that they can be traced to the distances of 2700 km, crossing the P_{520} phase.

Thus, both the first and secondary arrivals indicate regular stratification of the upper mantle. In general, all of the main arrivals identified consist of many phase groups which characterise the corresponding boundaries as high reflective zones with thickness ranging from 10 to 20 km. Average velocity contrasts are not high at the boundaries (0.0–0.1 km/s) but they are high within the thin

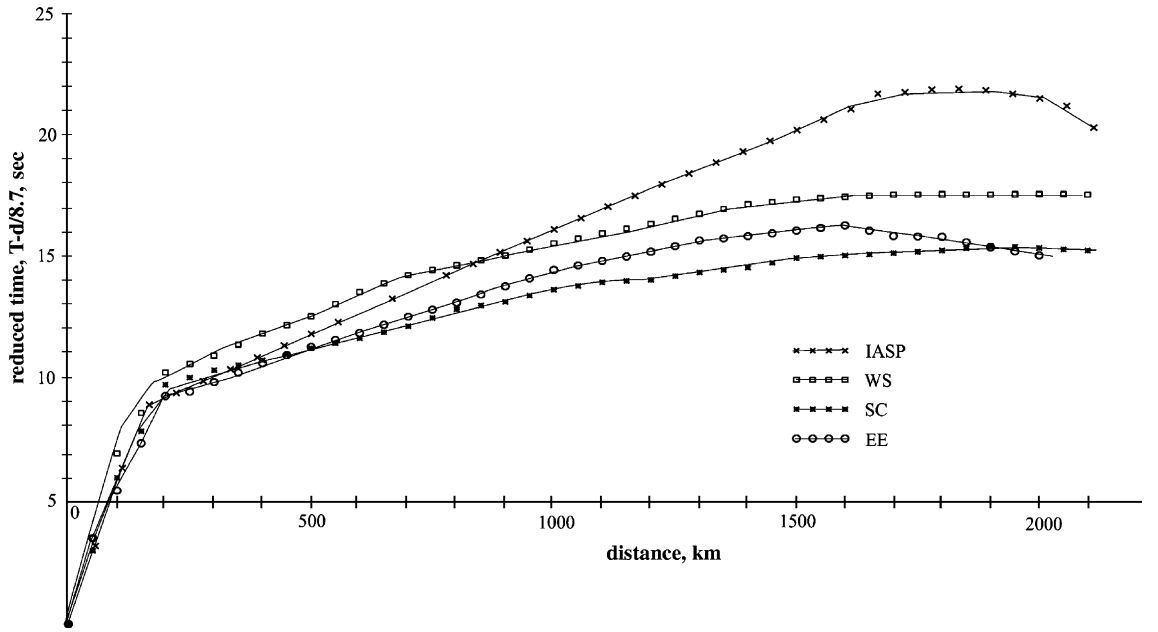

Fig. 4. Regional travel-times of the first arrivals for the East-European Platform (EE), West-Siberian Plate (WS) and Siberian Craton (SC) in comparison with IASP-91 times. Reduction velocity is 8.7 km/s. The EE regional travel-times were constructed as average from the travel-times, recorded along Fennolora and Globus profiles, from SP Q1 with observation to the north and from the White Sea Shot (WS). The WS travel-times were determined from PNEs Q2, Q3, H1, H2, C1, C2 and C3 data. The Siberian Craton regional travel-times (SC) were determined from the profiles Rift, Meteorite and Kimberlite data.

layering. The P_{N2}, and P_L phases feature the largest amplitudes.

The travel-times of the principal phases constrain a basic model for the upper mantle of the study area. The model includes five layers limited by the following boundaries: N1 (with velocity V=8.35 km/s and depth interval D=70–120 km), N2 (V=8.4 km/s, D=100–130 km), L (V=8.5 km/s, D=200–230 km) and H (V=8.6 km/s, D=300–330 km). The boundary velocities differ from the wave velocities due to the effect of the Earth surface curvature. The velocities increase linearly within the layers. Besides clear stratification of the upper mantle, the observed travel-times show regular velocity variations over the area. They may be divided in three regional travel-times which correlate with the tectonic domains: the East-European group, the Siberian Craton group and West-Siberian group (Fig. 4).

The East-European regional travel-times (EE) were constructed averaging the travel-times, recorded along the Fennolora and Globus profiles, from SP Q1 with observation to the north and from the White Sea Shot (WS). All these profiles are located inside the East-European Platform and characterise only this platform. They form a compact group of the observed times which indicates similarities in the crust and upper mantle structure of the platform at different parts.

The West-Siberian regional travel-times (WS) were constructed averaging times from SPs Q2 and Q3 of the Quartz profile and from the reversed shots H1 and H2 of the Horizont profile. They characterise two young platforms: the West-Siberian and the Timan-Pechora. Later, the WS times were completed using data from SPs C1, C2 and C3 of the Craton profile.

The WS travel-times differ from those of the EE by a 1.0–1.5-s delay of the first arrivals at offsets of 200–1500 km and by a shift of P_N and P_L arrivals towards larger times. This time delay is most probably due to the low velocity sediments in West Siberia. The relative WS time increase, observed at distances of 200–700 km, is due also to a decrease in first arrival velocities of 8.1–8.2 km/s in comparison with that of 8.1–8.3 km/s for the EE group.

The Siberian Craton regional travel-times (SC) were determined from the Rift, Meteorite and Kimberlite profiles. They differ from the EE and WS travel-times by higher velocities (8.3–8.5 km/s) of the first arrivals within offset ranges of 200–1700 km.

The IASP-91 travel-times differ from all regional travel-times, mainly, the P_N phase features lower velocities. As a result, time delays of 2–5 s are observed between IASP-91 and all regional travel times at the distances of 1000–2000 km (Fig. 4).

3. 2-D velocity modelling

A ray-tracing method was used to build the upper mantle model. This method is very flexible and has no limitation on the model type or number of phases. It is also useful for the determination the origin of the seismic phases and for studying the possible non-uniqueness of the solution. Our experience shows, however, that the ray-tracing results and the reliability of the resulting velocity model are strongly depend upon the starting model. Thus, the most important stage of the DSS data interpretation is the construction of reliable starting models. In this study, these models have to include the boundaries described above. There are different ways to obtain a starting 2-D model. Many authors compile it from a set of 1-D models determined from each record section. This approach is dangerous because in 1-D modeling the horizontal inhomogeneities might produce many unrealistic local velocity anomalies that are difficult to exclude from the final 2-D model due to poor or irregular ray coverage. The 1-D models are useful only if they are determined from regional travel-times averaging of similar phases for horizontally homogeneous blocks.

In order to constrain the main tendencies in the lateral variation of the velocities, we analysed the reversed and overlapping travel times. First, we removed the influence of the near surface and crustal inhomogeneities from the travel-times of the mantle phases. For that propose, the reversed and overlapping travel-times are compared to reveal the time delays observed from different shot-points at the same intervals within the profile. These time delays are connected with surface inhomogeneities and they are not used in the starting model construction.

Additionally, to better constrain the starting model we used the intercept-time method (Pavlenkova, 1982; Pavlenkova et al., 2002), in which the observed refraction and wide-angle reflection travel times are reduced with different reduction velocities Vr and placed to the midpoints between source and receiver. The envelopes of such travel-times are the intercept time curves $t_i=f(x,\mathrm{Vr})$ which can be transform to the depth to the velocity level $V=\mathrm{Vr}$. The time sections give realistic pictures of the 2-D velocity structure. This method also provides information on the nature of the secondary arrivals: the reflection travel-times which correspond to the boundary with the velocity $V=\mathrm{Vr}$, coincide with the curve $t_i(\mathrm{Vr},x)$ at the critical points.

In Fig. 5, an example is given for the Kimberlite data set interpretation using this methodology. The travel-times reduced by Vr=8.5 km/s were transformed to midpoints. The t_i curve characterises the form of the N2 boundary showing an uplift of the boundary beneath the Siberian craton. Near the velocity level V=8.5 km/s there are two good reflectors, the high amplitude secondary arrivals P_{N1} and P_{N2} (Fig. 5a). Once the starting model was build, it was improved by forward ray tracing.To control how reliable the main boundaries are and how stable the velocities are between them, the velocity cross-sections were determined by ray tracing, independently, along each profile. The boundaries were modelled without changing the velocities along them. If the main boundaries were not sufficient to describe the velocity structure, some additional boundaries were included in the models. In some cases, the N boundary velocities were also changed but not more than in 0.05 km/s.

Then the parameters of the basic layers (the layer velocities and their depths) determined along the profiles were compared at the profile intersection points. The comparisons showed that the velocities differed only within +0.05 km/s. In general, the depths to the boundaries at the intersection points differ at most by 10 km, which is a good agreement indicated the validity of the principal layer determination. When intersection points are located at the edges of transects the depth differences sometimes reached 20–30 km, at this location the lack of subsurface coverage prevents a reliable determination of the velocities. Another cause for depth differences at intersection points can be due to the complex waveforms, phases identified in different profiles might not correspond to the same interface. Time differences between phases 0.4–0.6 s and ray tracing indicate that the corresponding depth differences may be up to 20 km. To exclude such cases the records and cross-sections were analysed once more and addition-

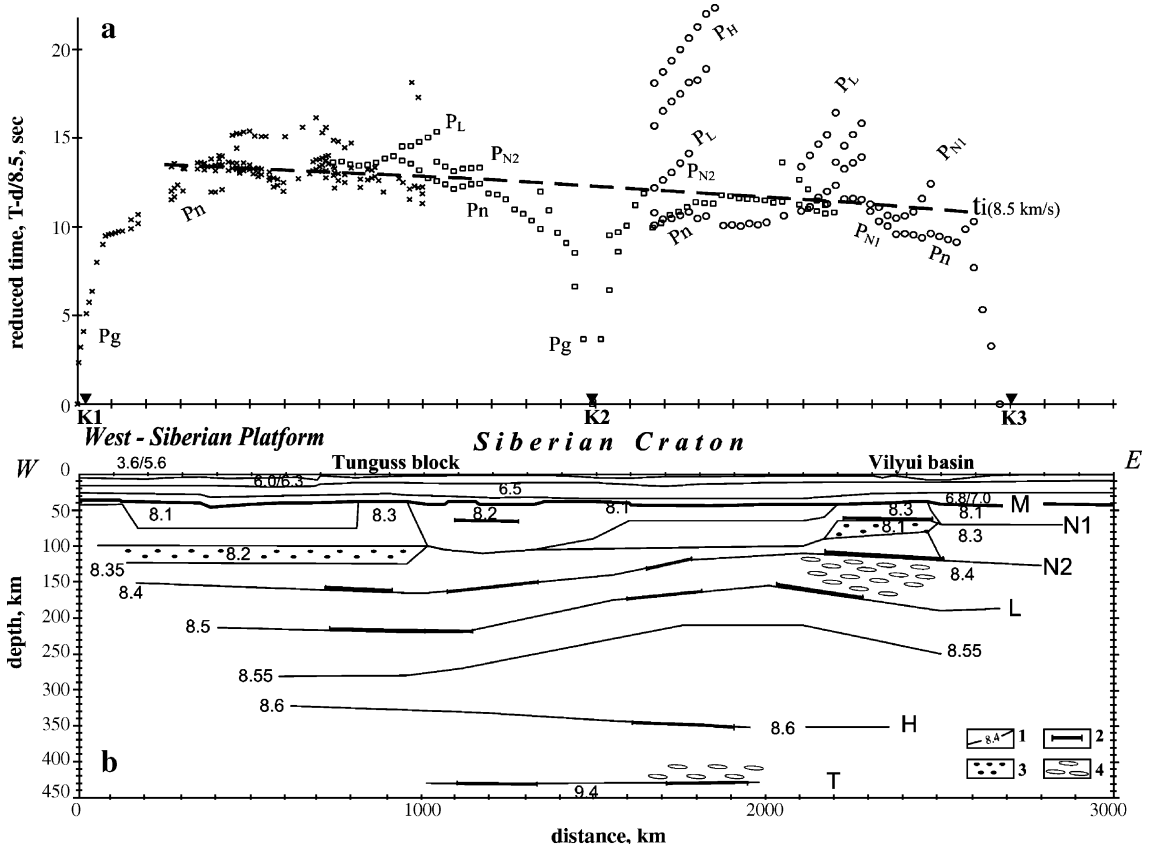

Fig. 5. (a) Reduced and transformed to midpoints travel times of the basic mantle waves recorded along the profile Kimberlite. Reduction velocity Vr=8.5 km/s. Dashed line $t_i(x)$ is the intercept times for the velocity level V=8.5 km/s. See legend in Fig. 2. (b) Velocity cross-section along the profile Kimberlite. K1, K2 and K3 are PNE locations. (1) Seismic boundaries with constant velocity (the velocities increase linearly between the boundaries, (2) reflectors generated high amplitude waves, (3) low velocity layer, (4) high reflectivity zone.

al ray tracing was carried out to obtain agreement between the models at their cross-points.

3.1. Kimberlite profile

The Kimberlite profile crosses the Siberian Craton and the eastern part of the West-Siberian Plate (Fig. 1). This profile features three shot points. Some chemical explosions also feature mantle arrivals up to 400–600 km offsets.

The first arrivals of the mantle phases show higher velocities than in the other profiles (Fig. 3). The secondary waves are not so strong on the Kimberlite profile; we determined, however, P_{N1}, P_{N2}, P_L and P_H. The largest velocity variations are observed in the upper 150 km of the mantle: (from 8.1–8.2 km/s to 8.3 km/s) in two high velocity blocks: at the boundary between the craton and the West-Siberian Platform (Tunguss block) and, in the Vilyui Basin area (Vilyui block). In the western part of the profile at depth of 100–120 km, a low velocity zone is detected. A velocity inversion is also outlined beneath the Vilyui high velocity block.

At depths of 100–250 km, a clear difference is observed in the mantle structure between the Siberian Craton and West-Siberian Platform. The envelope of the reduced travel-times that correspond to the velocity level 8.5 km/s (the N2 boundary) shows a time decrease from west to east (Fig. 5a), which indicate an uplift of the N2 boundary. Similar structure is found for the N1 and L boundaries (Fig. 5b). At a depth of 300 km, the situation changes: the H boundary depth increases beneath the craton. To describe this structural change, an additional boundary is included in the model with $V = 8.55$ km/s.

3.2. Craton profile

The Craton profile also crosses the Siberian Craton and the eastern part of the West-Siberian Platform (Fig. 1). Four PNEs were recorded along the profile providing information of the whole upper mantle, and the mantle transition zone (Figs. 2 and 3, RNEs C1, C2 and C4). In the eastern part of the profile, several chemical explosions were recorded at offsets up to 600–700 km.

The resulting model also displays the largest velocity variations within the upper 120 km of the mantle (Fig. 6). The N1 boundary is located at 130 km depth in the western part of the profile and only 80 km in the eastern part. The low velocity region covers the West-Siberian Plate and the eastern part of the Siberian Craton. High velocities are observed in the Vilyui basin area. The N2 and L boundaries uplift from the west to the east too but the uplift values decrease with depth. The H boundary has an opposite geometry: it dips towards the east. Thus, the velocity cross-section along the Craton profile in general is similar to that of the Kimberlite profile. There are, however, some differences. The Tunguss high velocity block is not distin-

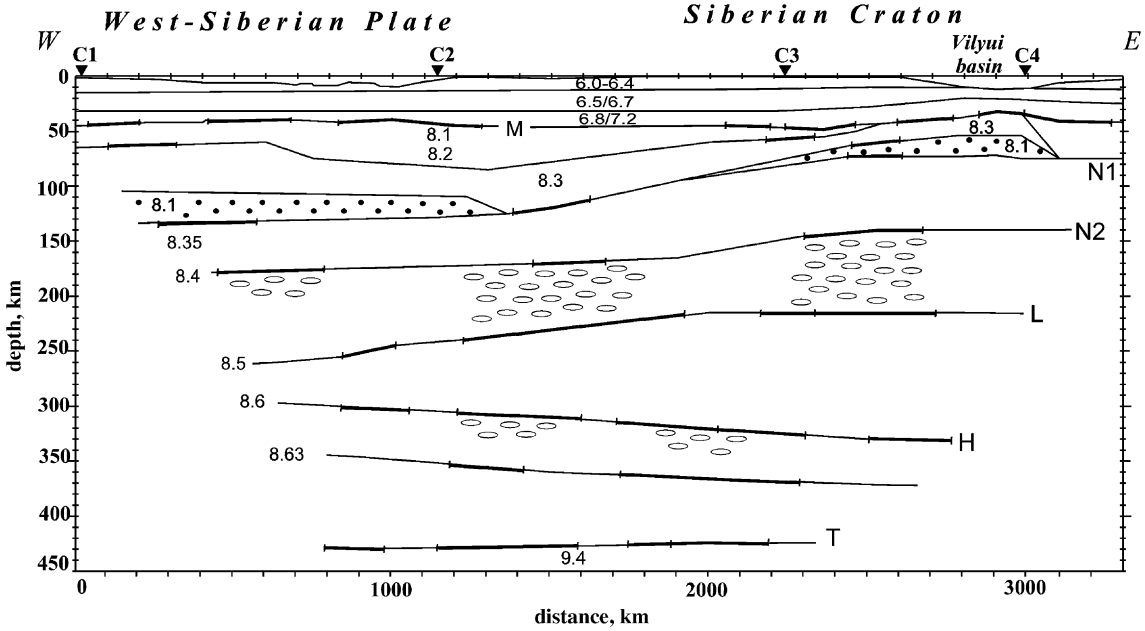

Fig. 6. Velocity cross-section along the profile Craton. See legend in Fig. 5b.

guished on the Craton profile. In contrary in this part of the profile, the uppermost mantle velocities are lower than in other area of the craton. This indicates the mantle structure to change in the central part of the craton, and not beneath its margin.

3.3. Meteorite profile

The Meteorite profile crosses the Siberian Craton from north to south, from the Taimir Orogen Belt to the Baikal Rift Zone (Fig. 1) and consists of 4 PNEs.

On the Meteorite profile only the Pn waves are recorded as stable first arrivals. The apparent velocities of these waves (8.2–8.4 km/s) are higher than in the other profile. At offsets of 700–1000 km, Pn attenuate and at larger distances the first arrivals are weak (RNE M4 in Fig. 2). The secondary arrivals are complex and wave correlation is more difficult than on the other profile.

Nevertheless, a minimum structure model was determined (Fig. 7). Again the largest velocity variations are observed in the upper 100 km of the cross-section above the N1 boundary. Two high velocity blocks can be identified in the central and southern parts of the Siberian Craton. They are identified from reversed and overlapping travel-times showing an increase of the velocities up to 8.4 km/s in the same intervals of the profiles. It is the Tunguss block that was revealed by the Kimberlite profile and the Pre-Baikal block. In the other portions of the profile, the average uppermost mantle velocities are 8.1–8.2 km/s. Similar to the other profiles at depth of 80–100 km a low velocity layer is distinguished along the northern part of the Meteorite profile.

The N boundaries show uplift beneath the Siberian Craton (Fig. 7). The L boundary also shallows from north to south but only to 1600 km of the profile, suggesting a subsidence beneath the N2 boundary uplift (1900–2400 km of the profile). The depths of the H boundary are stable along the Meteorite profile, although there is a small dip to the south.

3.4. Rift profile

The Rift profile crosses the northern part of the West-Siberian Platform (in area of the deep Pur-Gidan Basin), western part of the Siberian Craton and, the Baikal Rift Zone (Fig. 1). Three PNEs were shot during the experiment (Cipar et al., 1993; Priestly et al., 1994; Pavlenkova et al., 2002).

Two regions of anomalous high sub-Moho velocity (8.4 km/s) are distinguished by this profile: the Tunguss block and the Pre-Baikal block. Beneath the Tunguss block, the reversed travel-time curves show first arrival apparent velocities of 8.4 km/s. The Pn wave from PNEs R1, R2 and R3 have similar high velocities in this region. The high sub-Moho velocity of the Pre-Baikal block is seen in the Pn travel times from several chemical SPs as well.

The shadow zone observed between the Pn and P_N phases from SP R2 (Fig. 2) requires a velocity inversion

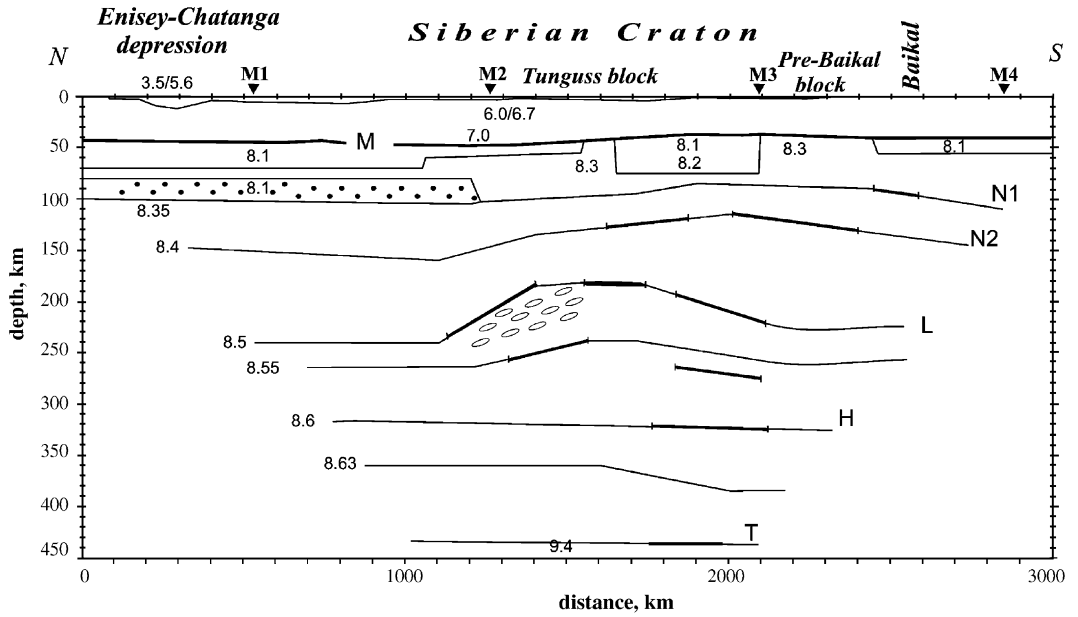

Fig. 7. Velocity cross-section along the profile Meteorite. See legend in Fig. 5b.

starting at about 80 km depth. The upper mantle structure beneath the low velocity zone is difficult to describe using the basic layers alone: thus, several intermediate boundaries are required and the velocities vary within them (Fig. 8). The most complex velocity structure is observed beneath the Tunguss block: the N2 and L boundaries uplift here and the velocities at this location are higher (0.1 km/s) than in the starting model. It suggests that in this area (at a depth of 100–250 km and at the profile interval 1000–1500 km) there is a shear zone with several reflectors dipping to the north. The zone generates reflections with anomalous high apparent velocities and complex wave pattern (Pavlenkova et al., 2002).

3.5. Quartz profile

The long-range Quartz profile crosses several large geological provinces: the East-European Platform, the Timan-Pechora plate, the Urals, the West-Siberian Platform and the Altai Mountains (Fig. 1). The profile includes 3 nuclear explosions (PNEs Q1, Q2, Q3 in Fig. 1) and several large chemical explosions. This profile is characterised by the high quality of the recordings and by the longest system of reversed and overlapping observations (Mechie et al., 1993; Morozov et al., 1999).

The upper mantle model (Fig. 9) again shows very pronounce velocity inhomogeneity in the uppermost mantle. The most complicated structure is observed beneath the Urals. Interesting features of the model in this region are the inclined, west dipping reflecting boundaries at depths of 50–100 km. They look like fault or shear zones divided the main tectonic domains: the East-European Platform, Timan-Pechora Plate and the Urals. Both faults dip to the east. In this area directly beneath the Moho, the velocities change from 8.0 to 8.4 km/s. Low velocities are determined beneath the Timan-Pechora Plate and the West-Siberian Platform and high velocities lie beneath the Urals. This difference, however, is observed only for the upper 30–40 km of the mantle. At a depth of 80 km, a velocity inversion makes the mantle structure of the Urals similar to that of the West-Siberian Platform.

The depth of the N1 boundary is 70–80 km in the East-European Platform, it increases down to 100 km in the Urals and to 130 km in West Siberian Plate. The N2 boundary is plainer: its depth is 130 km in the East European Plate and 160 km in the West Siberia. However, it strongly uplifts under the Altai Mountains. The L and H boundaries are near horizontal at approximate depth of 220 and 340 km, respectively.

3.6. Globus profile

The profile crosses the eastern part of the East-European platform and partly the Timan-Pechora

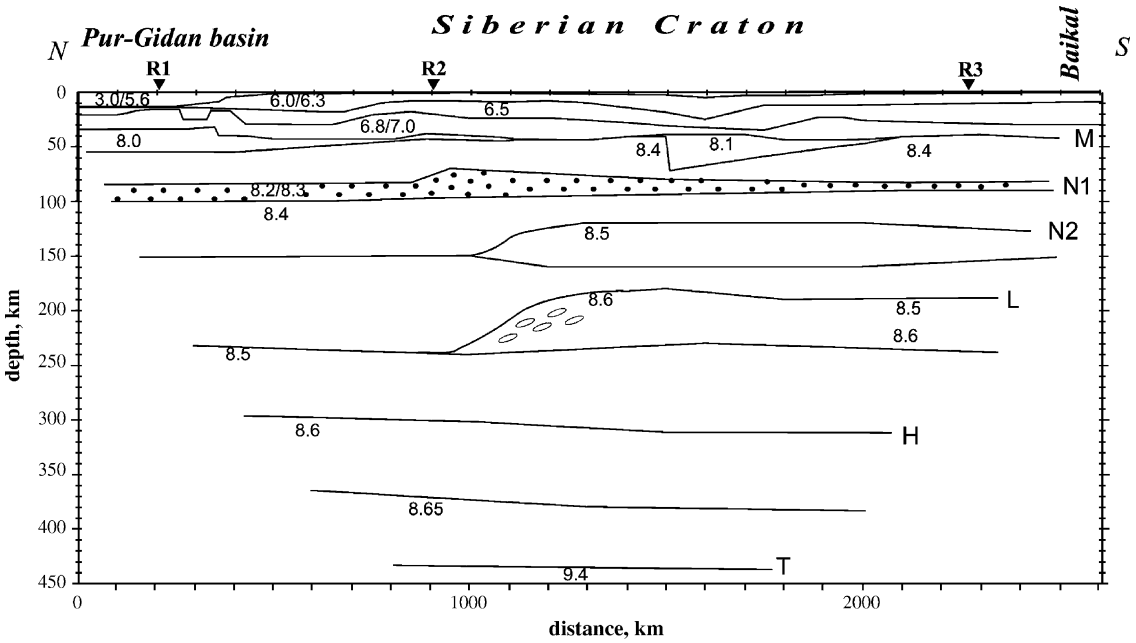

Fig. 8. Velocity cross-section along the profile Rift. See legend in Fig. 5b.

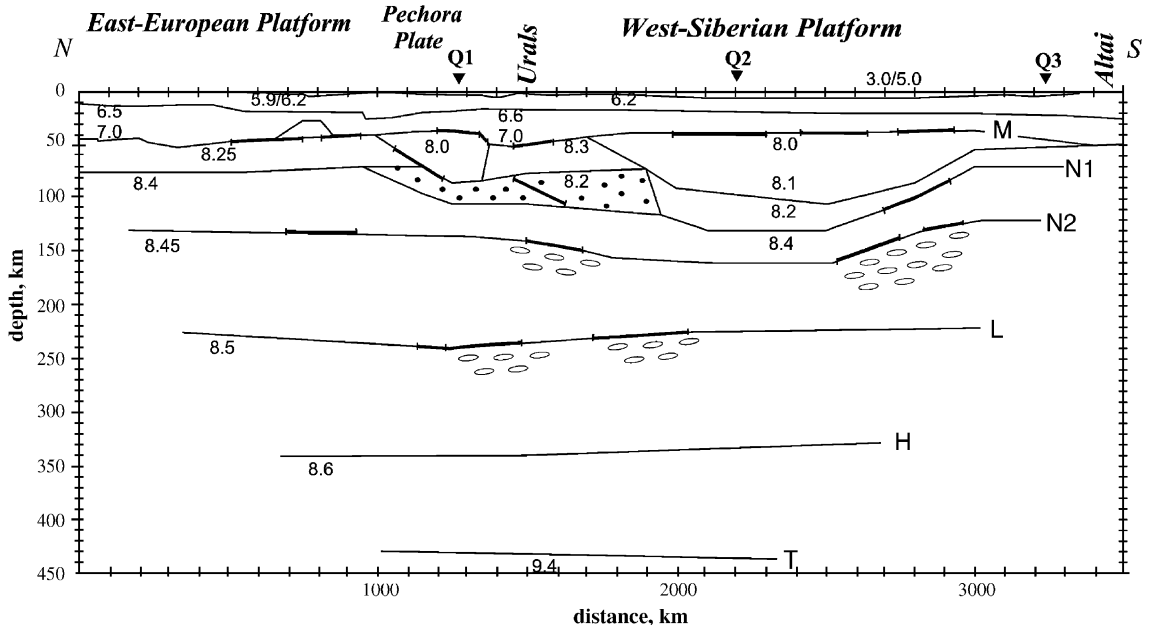

Fig. 9. Velocity cross-section along the profile Quartz. See legend in Fig. 5b.

Plate (Fig. 1). It is 1500 km long. Four PNEs were recorded with the distance of 400 km between shot-points. No chemical explosions were made along this first PNE profile. A characteristic feature of the Globus profile is small amplitude of the Pn arrivals and existence of P_{N1} as first arrivals at 200–600 km offsets. The upper mantle velocity structure does not show relevant variations along the profile (Fig. 10). The observed times of the mantle phases vary mainly due to the sediments and crustal structure variations. A regular increase of the velocities with depth is clearly observed from 8.15 beneath the Moho up to 8.3 km/s at the N1 boundary (depth of 70 km) and up to 8.4–8.5 km/s at the N2 boundary (depth of 120 km).

3.7. Horizont profile

The Horizont profile crosses the northern parts of the Urals, the northern West-Siberian Platform and the northern Siberian Craton from Vorkuta to Tiksi (Fig. 1). Four PNEs were made here and only some chemical explosions. The latter are irregularly spaced, and do not cover the western part of the profile. The longest observations were carried out from SPs H1 and H4 with offsets up to 1100 km. They served to penetrate the upper mantle only to depths of 140 km. Travel-times of the mantle phases vary mainly due to the sediment structure and the apparent velocities variation can be either reflect the mantle structure or the base-

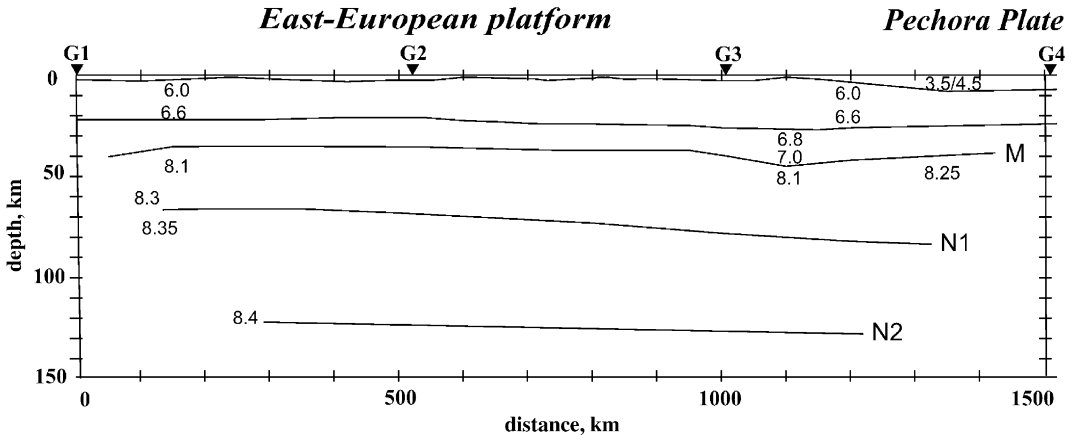

Fig. 10. Velocity cross-section along the profile Globus. See legend in Fig. 5b.

ment relief. However, three main phases were identified (the Pn, P_{N1} and P_{N2}).

In the western part of the profile, the uppermost mantle velocities are 8.0–8.1 km/s which are lower than these beneath the old platform (Fig. 11). The N1 boundary with velocity of 8.4 km/s is determined at the depth of 100 km shallows up to 70 km beneath the northern edge of the Urals. The N2 boundary with the velocity of 8.4 km/s is observed at the depth of 110–130 km. A low velocity zone is distinguished above the N1 boundary in the cratonic area.

3.8. Fennolora profile

The Fennolora profile crosses the Baltic Shield from south to north (Fig. 1). It is a part of the European Geotraverse and the seismic survey was carried out along the 1900 km profile with chemical explosions (Mueller and Ansorge, 1988). The longest observations were carried out from two shots (B and I) with offsets up to 1800–2000 km. They served to penetrate the upper mantle up to depths of 200 km.

This data set was interpreted by Guggisberg and Berthelsen (1987). A characteristic feature of their upper mantle model is thin layering with alternation of low velocity and high velocity zones. On the background of this complicated structure, it is difficult to see if there are any regular changes of the velocities along the profile or with depth. We have analysed all the experimental data and constructed a new and simpler cross-section which includes our basic model.

The mantle wave analysis shows a regular increase of the apparent velocities from 8.0–8.3 km/s which is typical of the Pn phase up to 8.4–8.5 km/s (P_N), and for P_L arrivals with velocities around 8.6 km/s. On this profile, it is difficult to divide P_N in two separate arrivals.

The model obtained clearly shows that the uppermost mantle structure changes from the north to south. The southern part of the profile is characterised by higher velocities beneath the Moho (up to 8.3 km/s). At depths of 80–100 km, a low velocity layer can be observed. This corresponds roughly to the low velocity layer identified by Abramovitz et al. (2002) from analysis of travel time picks of first arrivals. The bottom layer is a strong reflector, the N boundary. In the northern part of the profile, the uppermost mantle velocities are lower (8.1–8.2) and there are no clear velocity inversions. The velocities in the depth interval of 100–200 km are nearly constant along the entire profile.

3.9. Rubin profile

The Rubin profile has a dense system of the chemical explosions but only one PNE (SP Ru in Fig. 1). The mantle phases are recorded up to 1500 km offset. Large differences may be observed in the wave pattern between the Rubin and the other profiles. Weak Pn waves are not visible in the shot records, instead, the high amplitude reflections from the N1, N2 and L boundaries are characteristic for this profile. A peculiarity of the Rubin wave-field is the anomalously high apparent velocities of P_{N1} and P_{N2} phases: more than 9.0 km/s. As a result, the first arrival travel-times show a large negative anomaly at distances 700–1200 km relative to the other profile data.

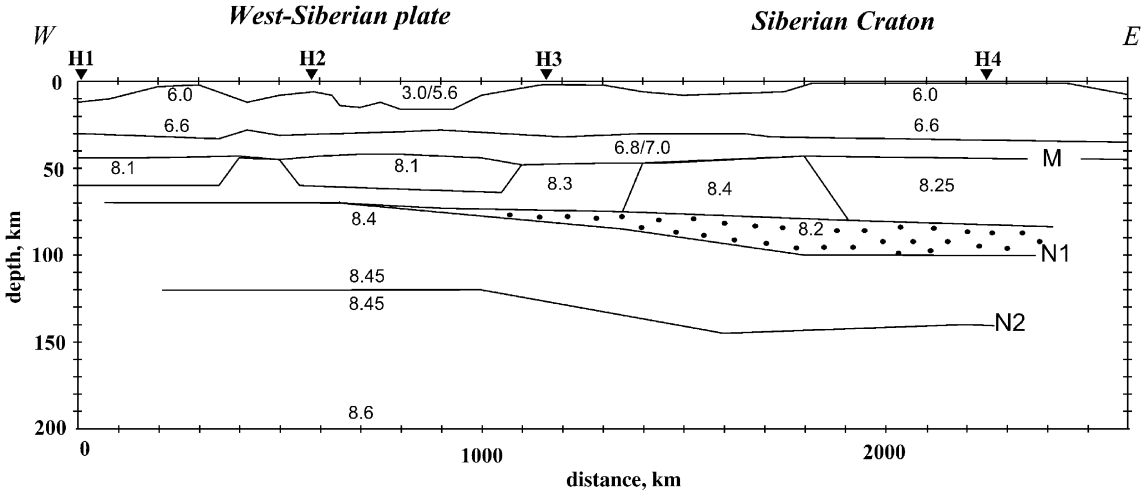

Fig. 11. Velocity cross-section along the profile Horisont. See legend in Fig. 5b.

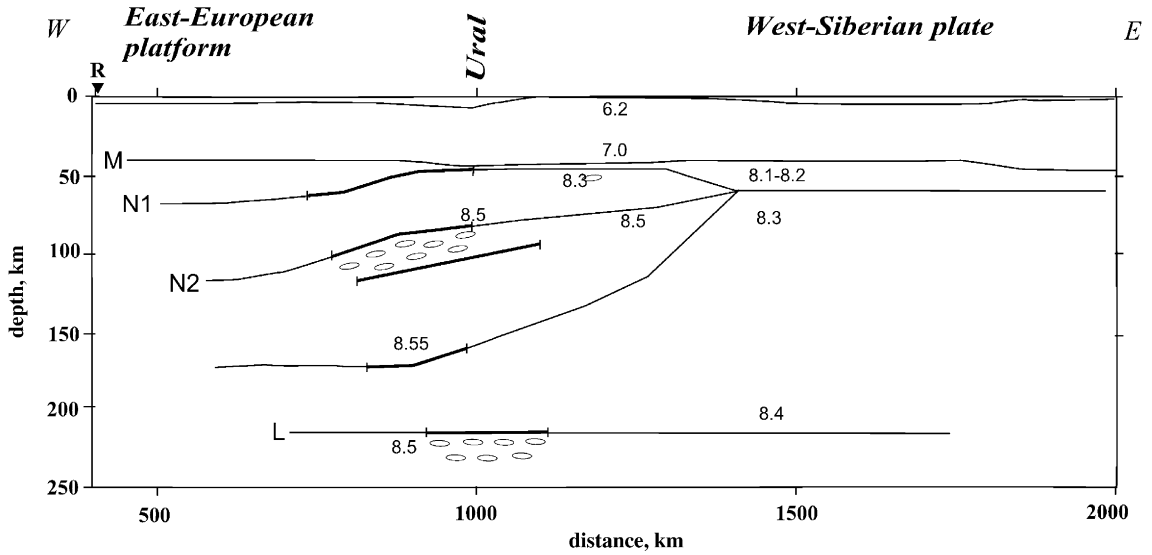

Fig. 12. Velocity cross-section along the profile Rubin. See legend in Fig. 5b.

To explain the observed wave pattern, two possible models were considered: the anomalous apparent velocities of P_N waves caused (1) by an increase of the mantle velocities in the central part of the profile and (2) by a inclination of the reflectors to the west. The better fit of travel time data was achieved by ray-tracing through the second model (Fig. 12). The first model required unrealistic high velocities for the uppermost mantle. The reflections from dipping boundaries may have very high apparent velocities. As shown in this

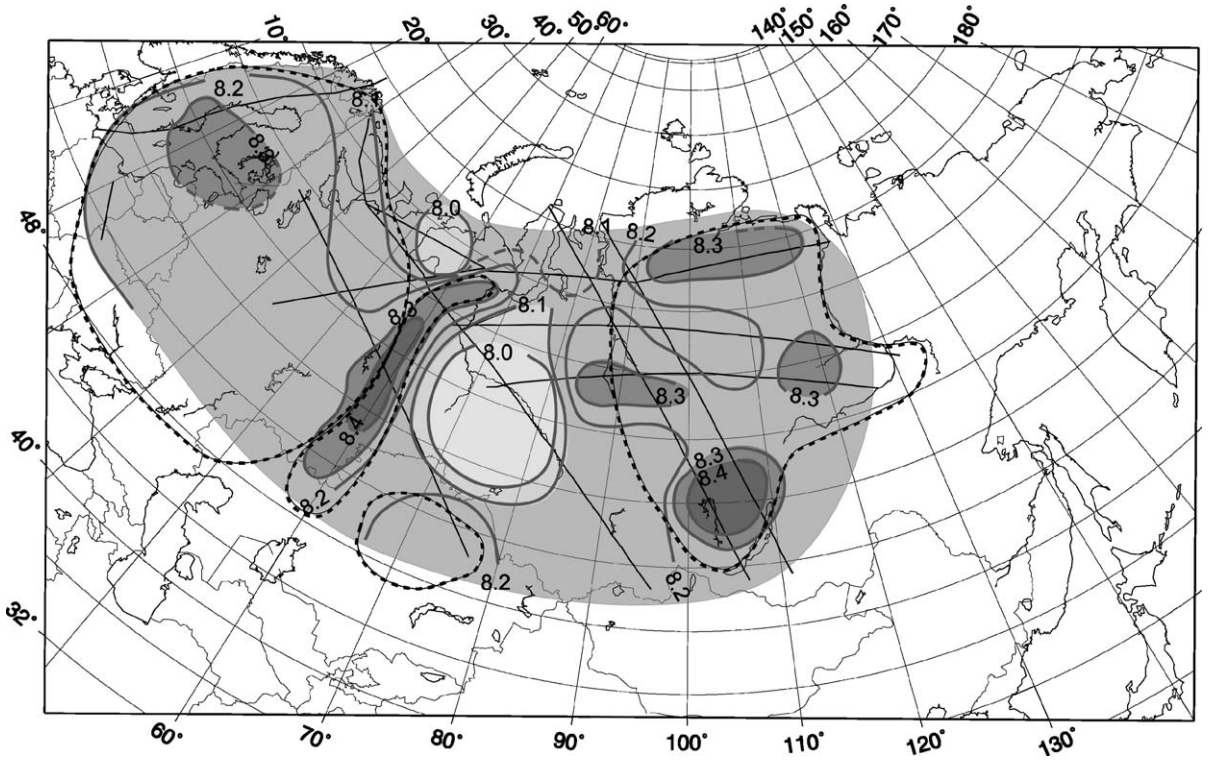

Fig. 13. Scheme of the uppermost mantle velocity distribution at depth of 60 km. Thin lines are the seismic profiles, dotted lines show the main tectonic units (Fig. 1).

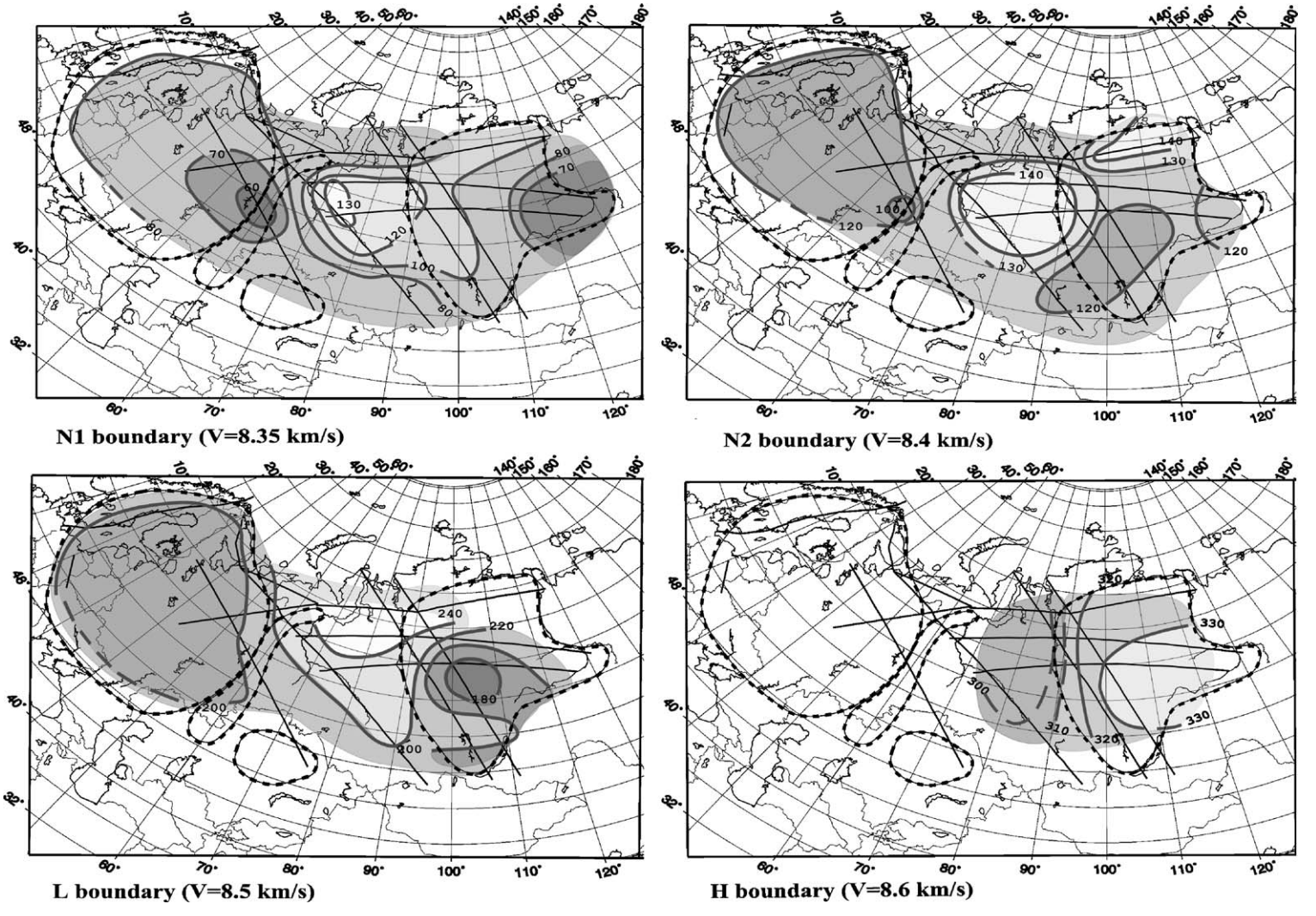

Fig. 14. Depth maps for the mantle boundaries N1 (boundary velocity is 8.35 km/s), N2 (8.4 km/s), L (8.5 km/s), H (8.6 km/s).

model, both the N1 and N2 boundaries shallow beneath the Urals. The dipping N1 and N2 boundaries generate reflections with apparent velocities up to 9 km/s. The L boundary is near horizontal.

4. 3-D velocity and structural model of the upper mantle

The number of the long-range seismic profiles in the study area is not enough to construct a well-resolved 3-D velocity upper mantle model (3-D velocity grid). However, the profile data can be used to compile simple structural maps.

The mantle structure can be described as velocity distribution at some depths and as depth maps for the main mantle boundaries. The first scheme reveals horizontal velocity inhomogeneities, the second reveals the trends and geometry of seismic boundaries in the study area.

To describe the completed velocity structure of the uppermost mantle, we constructed the map of the velocity distribution at a depth of approximately 60 km (Fig. 13). For deeper parts of the mantle, the 3-D model is presented in form of depth maps to the man boundaries N1, N2, L and H (Fig. 14). This unique data set sparsely samples the lithosphere of the Northern Eurasia. In order to obtain a reasonable 3D model for the upper mantle, and to be able to correlate from transect to transect, filing in the gaps, additional, geological and geophysical information was considered.

Therefore, some correlation of the uppermost mantle velocities with tectonics and geophysical fields can be emphasised. Low velocities are observed in the areas of high heat flow and in tectonic active areas. In the West-Siberian and Timan-Pechora Plates, likewise associated with young platforms, the mantle velocities are lower than in the adjacent ancient platforms. But this correlation is not so visible for the deeper parts of the upper mantle, where there is a reversal correlation between the shallow and the deep mantle boundaries: the H boundary is dipping if the N and L boundaries are rising (Figs. 6 and 14).

Beneath the Moho, the velocities change from 8.0–8.2 km/s in the West Siberia to 8.3–8.4 km/s in some blocks of the Siberian Craton and the Urals (Fig. 14). Four high velocity blocks are outlined in the Siberian Craton. Three of them are determined from the reliable data of the reversed profiles: (1) the Tunguss block crossed by the Meteorite, Rift and Kimberlite transects, (2) the Vilyui block in the western part of the Vilyui Basin sampled by the Craton and Kimberlite data and (3) the Pre-Baikal block in the southern part of the craton sampled by the Rift and Meteorite data. Although, the high velocities are also distinguished along the Horizont profile (Fig. 11) but they feature poor resolution.

High velocities are also typical for the uppermost mantle beneath the Urals. They are constrained along Quartz and Rubin profiles (Figs. 9 and 12). The East-European Platform mantle looks more homogeneous than that of the Siberian Craton. A local high velocity anomaly is observed beneath the Baltic Shield. Low velocities (8.0–8.1 km/s) are characteristic for the central part of West Siberia and of the Timan-Pechra Plate. In all the other regions, the velocities 8.1–8.2 km/s are observed.

At the depth of 100 km, the local high velocity anomalies disappear and only two large anomalies are observed (Fig. 14): (1) low velocities in the central part of the West Siberia and (2) and high velocities in the Middle Urals. These structural features follow from the depth map of N1 boundary. It is near 130 km depth in the central part of the West Siberian Plate and only 60 km deep in the Middle Urals.

The depth maps of the N2 and L boundaries show a similar patterns. The West Siberia region is characterised by low velocities. This is suggested by the depth map to the N2 boundary because it reach 140 km in this area. The eastern part of the Siberian craton features high velocities as indicated by the depth map to the N2 boundary as it shallows up to 120 km. There are, however, some differences. The L boundary clearly shows that the lower velocity area covers not only the West Siberian platform but also the northern part of the Siberian Craton as well. A high velocity zone is concentrated in the central part of the craton. The depth map of the H boundary shows the opposite pictures: larger depths beneath the eastern part of the craton (330 km) and the depths of 300 km beneath the West-Siberian platform (Fig. 14).

5. Discussion and conclusion

The 3-D model provides unique information to answer the following questions:

(1) What are the general changes of the upper mantle velocity structure and how do they correlate with tectonic regimes and geophysical fields?
(2) Are there any regional seismic boundaries in the upper mantle and what are their origins?
(3) What is the lithosphere–asthenosphere system beneath different tectonic domains of the Northern Eurasia?

The model presented shows that the upper mantle is characterised by the strong horizontal inhomogeneity. This complexity is manifested by changes in seismic velocities, by the degree and nature of layering and by the relief of seismic boundaries. In the uppermost mantle, these changes often occur not gradually but suddenly indicating a block structure.

In general, the mantle structure reflects a correlation with tectonics but the correlation is different for the different depth ranges. The East-European Platform and the Siberian Craton have higher velocities in the uppermost mantle as regards the younger West-Siberian and Timan-Pechora platforms. The Urals are also characterised by high velocities beneath the Moho but their deeper structure is closer to the West-Siberian platform. The velocity differences between small tectonic futures are observed down to 100–120 km, and between large tectonic domains—down to 200–250 km. The deeper mantle is more homogeneous.

A correlation between geophysical fields and upper mantle structure is also observed in the study area and it also changes with depth. Close correlation is determined between the uppermost mantle velocities and the heat flow. In the areas with low heat flow, the upper mantle velocities are higher. The higher heat flow regions are correlated with the lower mantle velocities.

These general correlations, however, are not observed in the inner parts of the Siberian Craton. The upper mantle velocities show differences in structure between the northern and southern portions of the craton although there are no differences between these areas in geological history or heat flow fields. At depth lager than 100 km, the northern part of the craton is characterised by lower velocities similar to the West Siberian ones. This may be explained by contemporaneous geodynamic activation of the northern part of the craton. The activation covers a portion of the mantle too deep to be seen in the surface heat flow. It might be a result of influence of the tectonically active Arctic region. It is important geodynamic conclusion. Note that the Baikal active zone has little influence on the upper mantle of the Siberian Craton.

Specific features of the Siberian Craton structure are the high velocity blocks in the uppermost mantle (Fig. 13), which cannot be correlated to other geophysical observation. Anomalously high velocities were distinguished earlier in other parts of the craton and their nature has been discussed elsewhere (Pavlenkova et al., 1996; Suvorov et al., 1999). The main conclusion was that such velocities could not be explained by a general change in mantle composition (Sobolev and Fuchs, 1993). The most plausible explanation for them is seismic anisotropy which is typical of the upper mantle (Fuchs, 1983; Babuska et al., 1984). The high velocities may be related the stress distribution or results of mantle flow patterns during the formation of the craton. Although, other explanations are possible. The high velocities in some uppermost mantle blocks may indicate the lost of iron during large basalt effusions in the craton area.

From the data analysed, the upper mantle is clearly stratified. Besides the velocity layering the regional reflecting boundaries are traced in the large area of the Northern Eurasia. They are characterised by stable boundary velocities. Those are N1 boundary (the boundary velocity 8.35 km/s), N2 (8.4 km/s), L (8.5 km/s) and H boundary (8.6 km/s). This is an unexpected result because several regular and strong enough velocity contrasts are revealed in the upper mantle where no phase transitions are predicted (Griffin et al., 1998). The mantle reflections are distributed irregularly in the time–distance scales, and it might suggest irregular space distribution of correspondent reflectors. The most reflectors, however, coincide with concrete velocity discontinuities.

The velocity contrasts at the boundaries are not more than 0.1 km/s (it is the maximal difference of the average velocities between the main layers), but the reflections are very strong. It can be proposed that the boundaries are 10–20-km-thick zones with alternation of high and low velocity layers. Such zones can be responsible for the high amplitude of many phase groups (Perchuc and Thybo, 1996; Thybo and Perchuc, 1997).

The origin of such boundaries in the ‘thermal lithosphere’ is not clear and needs a special study. One possible explanation involves the concentration of fluids at certain PT-condition. The fluids change the mechanical properties of the material present; they initiate partial melting and metasomatism of the mantle material, which results in the velocity changes. Solov’eva et al. (1989) have shown that mantle xenoliths from some distinct depths exhibit hints of partly melting. These depths correlate with the reflectivity zones described above. The fluids and melting can initiate flow along rheologically weak layers which results in seismic anisotropy.

From structural point of view, the most interesting boundaries are N1 and L. The N1 boundary is located at depths of about 100 km (from 70 to 120 km in our case). This boundary has been observed in many other regions as well: it was called the N boundary by Pavlenkova (1996b) and the 8^0 boundary by Thybo and Perchuc (1997). Thus, it may be considered to

have a global significance. The most important feature of the boundary is that it is a good reflector or reflectivity zone and it divides the mantle lithosphere in two portions with different inner structure. Above the boundary, the sub-Moho lithosphere is complex, laterally inhomogeneous, while beneath the N1 boundary the structure appears to be less complex (Figs. 5–12). Another specific feature of the boundary is that often it underlines low velocity layers. In the Baltic Shield, the velocity inversion is also characterised by higher electrical conductivity (Kovtun et al., 1994) suggesting the existence of fluids at this depth interval. Both characteristics indicate that the N1 or 8^0 boundary may be the bottom of the rigid part of the lithosphere and that beneath it the mantle material is more plastic and cannot preserve its own inhomogeneity.

A change of the mantle rheology is visible also at the L boundary. In many record-sections, the waves from this boundary attenuate and low velocity gradient zones may be proposed beneath the boundary. The Q factor that has been determined from the mantle wave spectrum (Egorkin, 1999) decreases at depth of 200–250 km. And, finally, an increasing of the plasticity at this depth interval follows from structural features of the L and H boundaries. The H boundary has a reversal form to the L boundary and it means that the material between the boundaries can flow to create isostatic equilibrium in the upper mantle.

The rheological stratification of the upper mantle does not agree with the classical "thermal model" of the lithosphere–asthenosphere system determined from the heat flow data. The lithosphere thickness outlined by a zone of possible solidus in the dry mantle is around 200–250 km beneath the old platforms (Kutas, 1984; Cermak, 1985). The seismic data have not revealed this asthenosphere which should be characterised by lower velocities. On the contrary, some hints of partly melted material may be suggested in the thin low velocity layers or in the high reflectivity zones traced as seismic boundaries.

The weak zones within the lithosphere should play an important role at any geodynamic process. They form a channel system for the mantle fluids, energy and material transportation. During tectonic activation, these zones are transformed into asthenolites (asthenolenses) by partial melting and may initiate mantle material intrusions into the crust.

Acknowledgments

This study was supported by the Russian Fund of Fundamental Investigations (RFFI), grant 04-05-64526. The record sections for the seismic profiles were kindly made available by GEON Centre of Russian Ministry of National Resource. We thank Karl Fuchs, Hans Thybo and colleagues for the useful discussions of the data and their interpretation methods. We are grateful to G.R. Keller for critical comments to a preliminary version of the paper and to his recommendations on how to improve the paper and also to the anonymous reviewer for valuable comments.

References

Abramovitz, T., Thybo, H., Perchuc, E., 2002. Tomographic inversion of seismic P- and S-wave velocities from the Baltic Shield based on FENNOLORA data. Tectonophysics 358, 151–174.

Babuska, V., Plomerova, J., Sileny, I., 1984. Spatial variations of P-residuals and deep structure of the European lithosphere. Geophys. J. R. Astron. Soc. 79, 363–383.

Beloussov, V.V., Pavlenkova, N.I., Kvjatkovskaya, G.N. (Eds.), 1991. Deep Structure of the USSR Territory (in Russian). Nauka, Moscow. 234 pp.

Benz, H.M., Huger, J.D., Leith, W.S., Mooney, W.D., Solodilov, L.N., Egorkin, A.V., Ryaboy, V.S., 1992. Deep seismic sounding in Northern Eurasia. EoS 73, 297–300.

Bulina, L.V., 1976. Characteristic features of the magnetic body bottom distribution in the USSR territory. Magnetic Anomalies Earth's Interior. Naukova Dumka, Kiev, pp. 137–151 (in Russ.).

Carbonel, R., Gallart, J., Perez-Estaun, A., Diaz, J., Kashubin, S., Mechie, J., Wenzel, F., Knapp, J., 2000. Seismic wide-angle constraints on the crust of the southern Urals. J. Geophys. Res. 105 (B6), 13755–13777.

Cermak, V., 1985. Thickness of the lithosphere of the USSR territory from geothermal data. Geol. Geophys. 5, 33–40.

Cipar, J.J., Priestley, K., Egorkin, A., Pavlenkova, N., 1993. From rift to rift: the Yamal Peninsula–Lake Baikal deep seismic sounding profile. Geophys. Res. Lett. 20, 1631–1634.

Druzhinin, A.S., Karatin, Yu.S., Ribalka, V.M., Khalevin, N.I., 1981. New data on deep structure of the Urals. Dokl. AN USSR 258 (1), 173–176.

Egorkin, A.V., 1997. Evidence for 520-km discontinuity. In: Fuchs, K. (Ed.), Upper Mantle Heterogeneities from Active and Passive Seismology. Kluwer Acad. Pub., Dordrecht, pp. 51–61.

Egorkin, A.V., 1999. Study of the mantle by superlong geotraverses. Phys. Earth 7–8, 114–130.

Egorkin, A.V., Chernyshov, N.M., 1983. Peculiarities of mantle waves from long-range profiles. J. Geophys. 54, 30–34.

Egorkin, A.V., Zuganov, S.K., Pavlenkova, N.A., Chernyshev, N.M., 1987. Results of lithosphere studies from long-range profiles in Siberia. Tectonophysics 140, 29–47.

Fuchs, K., 1983. Recently formed elastic anisotropy and petrological model for the continental subcrustal lithosphere in southern Germany. Phys. Earth Planet. Inter. 31, 93–118.

Fuchs, K. (Ed.), 1997. Upper Mantle Heterogeneities from Active and Passive Seismology, NATO ASI Series (1. Disarmament Technologies—vol. 17), Contribution No. 336, International Lithosðhere Program. Kluwer Academic Publishers, Dordrecht. 366 pp.

Griffin, W.L., O'Reilly, S.Y., Ryan, C.G., Gaul, O., Ionov, D., 1998. Secular variation in the composition of subcontinental lithospheric mantle. In: Braun, J., et al., (Eds.), Structure and Evolu-

tion of the Australian Continent, AGU Geodynam. Ser., vol. 26, pp. 1–25.

Guggisberg, B., Berthelsen, K., 1987. A two-dimensional velocity model for the lithosphere beneath the Baltic Shield and its possible tectonic significance. Terra Cogn. 7, 631–638.

Kovtun, A.A., Vagin, S.A., Vardanyants, I.L., Kovkina, E.L., Uspenskii, N.I., 1994. Magnetotelluric sounding of the crust and mantle structure in the eastern Baltic Shield. Phys. Earth 3, 32–36.

Kutas, R.I., 1984. Heat flow, radiogenic heat, crustal thickness in the south-west of the USSR. Tectonophysics 103, 167–173.

Mechie, J., Egorkin, A.V., Fuchs, K., Riberg, T., Solodilov, L.N., Wenzel, F., 1993. P-wave mantle velocity structure beneath Northern Eurasia from long-range recordings along the profile QUARTZ. Phys. Earth Planet. Inter. 79, 269–286.

Morozov, I.B., Morozova, E.A., Smithson, S.B., Solodilov, L., 1999. Heterogeneity of the uppermost mantle beneath Russian Eurasia from the ultralong-range profile Quartz. J. Geophys. Res. 104 (B9), 20-329–20-348.

Mueller, St., Ansorge, J., 1988. Deep seismic sounding of the mantle lithosphere. In: Nolet, G., Dost, B. (Eds.), European Geotraverse (EGT) Project, the Upper Mantle. ESF, Strasbourg, pp. 63–76.

Nielsen, L., Thybo, H., Solodilov, L., 1999. Seismic tomographic inversion of Russian PNE data along profile Kraton. Geophys. Res. Lett. 26, 3413–3416.

Pavlenkova, N.I., 1982. The intercept-time method: possibilities and limitations. J. Geophys. 51, 85–95.

Pavlenkova, N.I., 1996a. Crust and upper mantle structure in Northern Eurasia from seismic data. In: Dmowska, R., Saltzmann, B. (Eds.), Advances in Geophysics, vol. 37. Academic Press, Inc.

Pavlenkova, N.I., 1996b. General features of the upper mantle stratification from long-range seismic profiles. Tectonophysics 264, 261–278.

Pavlenkova, N.I., Pavlenkova, G.A., Solodilov, L.N., 1996. High seismic velocities in the uppermost mantle of the Siberian craton. Tectonophysics 262, 51–65.

Pavlenkova, G.A., Priestly, K., Cipar, 2002. 2-D model of the crust and uppermost mantle along Rift profile, Siberian craton. Tectonophysics 355, 171–186.

Perchuc, E., Thybo, H., 1996. A new model of Upper mantle P-wave velocity below the Baltic Shield: indication of partial melt in the 95 to 160 km depth range. Tectonophysics 253, 227–245.

Pollack, H.N., Hurter, S.J., Johnson, J.R., 1993. Heat flow from the Earth's interior: analysis of the global data set. Rev. Geophys. 31, 267–280.

Priestly, K., Cipar, J., Egorkin, A.V., Pavlenkova, N.I., 1994. Upper mantle velocity structure beneath the Siberian Platform. Geophys. J. Int. 118, 364–378.

Riberg, T., Wenzel, F., Mechie, J., Egorkin, A., Fuchs, K., Solodilov, L., 1996. Two-dimensional velocity structure beneath Northern Eurasia derived from the super long-range seismic profile quartz. Bull. Seismol. Soc. Am. 86, 857–867.

Sobolev, S.V., Fuchs, K., 1993. Seismic velocities and density in the deep continental lithosphere from the composition of xenoliths. Terra Nova 5, 333–334 (Abstract suppl. 1 EUG V11, Strasbourg).

Solov'eva, L.V., Vladimirov, B.M., Kiselev, A.I., Zavijalov, L.L., 1989. Two stages of mantle metasamatites of deep xenoliths from Yakutia kimberlites and their relation to lithosphere processes. Precambrian Metasamotites and Their Ore Deposits. Nauka, Moscow, pp. 3–17 (In Russ.).

Suvorov, V.D., Parasotka, B.S., Cherny, S.D., 1999. Deep seismic studies in Yakutuya. Phys. Earth 7/8, 94–113.

Thybo, H., Perchuc, E., 1997. The seismic 8^0 discontinuity and partial melting in continental mantle. Science 275, 1626–1629.

Thybo, H., Perchuc, E., Pavlenkova, N.I., 1997. Two reflectors in the 400 km depth range revealed from peaceful nuclear explosion seismic sections. In: Fuchs, K. (Ed.), Upper Mantle Heterogeneities from Active and Passive Seismology. Kluwer Acad. Pub., Dordrecht.